Biochemical and Biophysical Research Communications 433 (2013) 24–30

Contents lists available at SciVerse ScienceDirect

Biochemical and Biophysical Research Communications

journal homepage: www.elsevier.com/locate/ybbrc

Repression of bone morphogenetic protein 4 by let-7i attenuates mesenchymal migration of head and neck cancer cells

Wen-Hao Yang [a], Hsin-Yi Lan [a], Shyh-Kuan Tai [e], Muh-Hwa Yang [a,b,c,d,*]

[a] Institute of Clinical Medicine, National Yang-Ming University, Taipei 11221, Taiwan
[b] Institute of Biotechnology in Medicine, National Yang-Ming University, Taipei 11221, Taiwan
[c] Cancer Research Center, National Yang-Ming University, Taipei 11221, Taiwan
[d] Division of Hematology-Oncology, Departments of Medicine, Taipei Veterans General Hospital, Taipei 11217, Taiwan
[e] Department of Otolaryngology, Taipei Veterans General Hospital, Taipei 11217, Taiwan

ARTICLE INFO

Article history:
Received 6 February 2013
Available online 26 February 2013

Keywords:
BMP4
let-7i
Mesenchymal migration

ABSTRACT

The movement modes of epithelial cancer cells in three-dimensional (3D) environments include the mesenchymal mode, which is associated with local invasion, and the amoeboid mode, which facilitates distant metastasis. The migratory behavior of individual cancer cells is critical for tumor dissemination; however, the mechanism underlying regulation of the switch between movement modes is not clearly understood. For head and neck squamous cell carcinoma (HNSCC), local invasion is the major route of dissemination. We previously demonstrated that, in HNSCC cells, Twist1 represses let-7i expression to elicit mesenchymal-mode movement through activation of Ras-related C3 botulinum toxin substrate 1 (RAC1). In this study, we discover another important target gene of let-7i for regulating HNSCC migration. Using bioinformatic tools, we identified bone morphogenetic protein 4 (BMP4) as a candidate target of let-7i. Further experiments, including 3′-untranslated region (UTR) reporter assays, quantitative RT-PCR and western blotting, confirmed that BMP4 is a bona fide target repressed by let-7i. In the HNSCC cell line OECM-1, knockdown of BMP4 reduced mesenchymal-mode migration and invasion in 3D culture. In clinical HNSCC samples, let-7i expression was inversely correlated with BMP4 expression. Our results revealed that let-7i attenuates mesenchymal-mode migration of HNSCC cells through repression of a novel target, BMP4.

1. Introduction

Head and neck cancer, including cancers arising from the oral cavity, oropharynx, hypopharynx and larynx, is one of the leading causes of cancer-related deaths worldwide [1]. More than 90% of head and neck cancers are squamous cell carcinoma (HNSCC), which is associated with smoking, drinking and betel nut chewing [2]. The clinical characteristics of HNSCC are distinct from cancers originating from other tissues/organs: advanced HNSCC is often associated with severe destruction of surrounding tissues, and locoregional recurrence is the major pattern of treatment failure. When disease recurs, the response rate to treatment reduces significantly. Intriguingly, compared with other types of cancers, the frequency of distant metastasis in HNSCC is relatively low [3]. However, understanding of the unique mechanism responsible for HNSCC local invasion is limited.

The three-dimensional (3D) cultivation system represents the living microenvironment and is superior to traditional culture systems for studying the migration of cancer cells [4,5]. In 3D environments, epithelial cancer cells migrate using multi-cellular collective movement [6] or individual cell movement, the latter of which includes mesenchymal- or amoeboid-mode movement [7]. For mesenchymal-mode movement, the cells possess an elongated shape with protrusion, whereas cells moving in an amoeboid mode often reveal a round shape with membrane blebbing [8,9]. Recent studies have suggested that mesenchymal-mode movement is important for local invasion; by contrast, the amoeboid-mode movement directs distant metastasis [10]. However, knowledge concerning controlling the switch between mesenchymal and amoeboid movement is limited.

MicroRNAs (miRNAs) are small, non-protein-coding RNA molecules that repress gene expression at the posttranscriptional level by partially base-pairing to the 3′-untranslated regions (3′-UTRs) of target mRNAs [11,12]. The role of miRNAs in cancer metastasis has been highlighted recently [13,14]. We recently discovered that, in HNSCC, the epithelial–mesenchymal transition (EMT) inducer Twist1 promotes mesenchymal-mode movement through

* Corresponding author. Address: Institute of Clinical Medicine, National Yang-Ming University, No. 155, Sec. 2, Li-Nong St., Peitou, Taipei 112, Taiwan. Fax: +886 228235870.
E-mail address: mhyang2@vghtpe.gov.tw (M.-H. Yang).

0006-291X/$ - see front matter © 2013 Elsevier Inc. All rights reserved.
http://dx.doi.org/10.1016/j.bbrc.2013.02.076

repression of let-7i, a member of let-7 family microRNAs that are expressed during stem cell differentiation and that act as a tumor suppressor [15–17]. Repression of let-7i elicits mesenchymal-mode movement through activation of Ras-related C3 botulinum toxin substrate 1 (RAC1) [18]. In the present study, we further identified a novel let-7i target involved in regulating HNSCC migration in 3D environments. We found that bone morphogenetic protein 4 (BMP4), a TGF-β superfamily protein that plays a critical role in embryogenesis [19], is a target repressed by let-7i. Knockdown of BMP4 reduces mesenchymal-mode movement in HNSCC. The present study uncovers both a novel target of let-7i and a new function of BMP4 in cancer cells migration.

2. Materials and methods

2.1. Cell lines and plasmids

The human HNSCC cell line FaDu and the human embryonic kidney cell line HEK-293T were obtained from the Bioresource Collection and Research Center of Taiwan. The HNSCC cell lines OECM-1, CAL-27, Ca-9 and HSC-3 were provided by Dr. Cheng-Chi Chang (National Taiwan University). OECM-1 and FaDu were cultivated in Roswell Park Memorial Institute (RPMI)-1640 medium with 10% heat-inactivated fetal bovine serum (FBS), and HEK-293T, Ca-9, HSC-3 and CAL-27 were cultured in Dulbecco's Modified Eagle's Medium (DMEM) with 10% FBS. The shRNA vectors pLKO-sh-BMP4-1 (TRCN0000059143) and pLKO-sh-BMP4-2 (TRCN0000059144) were obtained from the National RNAi Core Facility of Taiwan (http://rnai.genmed.sinica.edu.tw/). An shRNA vector against luciferase (pLKO-sh-Luc) was used as a control for knockdown experiments. The let-7i expression vector pmCherry-let7i, let-7i neutralization vector pmCherry-spg-let7i and control vectors were previously described [18]. The full-length 3′-UTR of BMP4 (NM_001202.3) was cloned into pMIR-REPORTER to generate pMIR-BMP4-wt, and site-directed mutagenesis was used to generate the let-7i binding site-mutated pMIR-BMP4-mut. The stable cell lines OECM1-mCherry and OECM1-let7i were generated previously [18].

2.2. Analysis of microRNA and cDNA microarray data from the NCI-60 database

The miRNA and cDNA microarray data, completed with Affymetix HG-U133A and B chip platforms in 60 cancer cell lines (NCI-60), were downloaded from the CellMiner database (http://discover.nci.nih.gov/cellminer/) [20]. The heat map result presented in Fig. 1A was processed using dChip software (http://biosun1.harvard.edu/complab/dchip/).

2.3. RNA isolation, reverse transcription and real-time quantitative PCR analysis

Total RNA was isolated using TRIzol Reagent (Invitrogen Corporation, Carlsbad, CA), and miRNA was isolated using the miRNeasy Mini kit (QIAGEN, Hilden, Germany) according to the manufacturer's protocol. Reverse transcription was performed using random primers (Invitrogen Corporation, Carlsbad, CA) for mRNAs or using specific stem-loop oligonucleotides for miRNAs [21]. Real-time quantitative PCR was performed using the StepOnePlus real-time PCR system (Applied Biosystems Inc., CA). GAPDH was selected as an internal control for mRNA, and U6 non-coding small nuclear RNA was used as a control for miRNA expression. The results were calculated by the $2^{-\Delta\Delta CT}$ method. The sequence of primers used in the present study was previously described [18] except for BMP4 (forward, 5′-TGAGCCTTTCCAGCAAGTTT-3′; reverse, 5′-GCATTCGGTTACCAGGAATC-3′).

2.4. Western blot analysis

Cells were harvested and lysed in Cell Culture Lysis Reagent (Promega Corporation, Madison, WI). After centrifugation, the protein concentration of the supernatant was determined using the Pierce BCA Protein Assay Reagent (Thermo Fisher Scientific, Waltham, MA). The cell extracts were separated by sodium dodecyl sulfate–polyacrylamide gel electrophoresis, and then the separated proteins were transferred to PVDF membranes. The target proteins were probed with primary and HRP-conjugated secondary antibodies. Finally, the immunoblot signals were detected using Immobilon Western Chemiluminescent HRP Substrate (Millipore Corporation, Billerica, MA). The primary antibodies used in the current study were anti-BMP4 (#5163-1, Epitomics International Inc., Burlingame, CA) and anti-β-actin (A1978, Sigma–Aldrich Corporation, St. Louis, MO).

2.5. Lentivirus production and infection

Lentivirus production was performed in HEK-293T cells co-transfected with pCMVΔR8.7, pDVsVg (National RNAi Core Facility, Taipei, Taiwan) and pLKO-sh-Luc (or pLKO-sh-BMP4-1/2) by jetPEI (Polyplus-transfection SA, Illkirch, France). After 48 h, packaged virus was harvested to determine the concentration. OECM-1 cells seeded in 6-well plates were infected with 20-fold virus concentrates combined with 8 μg/ml polybrene (Sigma–Aldrich Corporation, St. Louis, MO) for 24 h, and then selected by puromycin (Sigma–Aldrich Corporation, St. Louis, MO) for 2 weeks.

2.6. Luciferase activity assay

The reporter constructs (pMIR-BMP4-wt/mut) were co-transfected into HEK-293T cells with pmCherry-let7i, pmCherry-spg-let7i or the control vector(s). A plasmid expressing the bacterial β-galactosidase gene (pCMV-βgal) was co-transfected in each experiment as an internal control to check the transfection efficiency. The relative luciferase activities were assayed and analyzed as previously described [22].

2.7. Cell culture on top of collagen and reconstruction of immunofluorescence images from confocal microscopy

The details of these experiments were previously described [18]. Briefly, the harvested cells were plated on top of collagen, and an appropriate amount of serum-containing culture medium added. For immunofluorescent staining of F-actin on collagen, we coated each well of the Lab-Tek® II chamber slide (#154461, Thermo Fisher Scientific, Waltham, MA) with 0.5 ml of the 1.7 mg/ml collagen solution, and then dispensed 5×10^4 cells on collagen, covered the cells with 0.5 ml of medium, and allowed the cells to adhere for 16 h. After incubation, the cells were fixed, permeabilized and stained with Alexa-488 coupled to phalloidin (Invitrogen Corporation, Carlsbad, CA). Single sections and sequential Z sections of images were captured by the laser confocal microscopy Olympus FV1000 (Olympus Corporation, Tokyo, Japan), and the images were analyzed using Olympus FV10-ASW 1.7 software. DAPI was used for nuclear staining.

2.8. Analysis of cell morphology

The area and perimeter of the cells were determined by the cell shape in phase contrast images using MetaMorph® software (Molecular Devices, Inc., Sunnyvale, CA). The morphology index

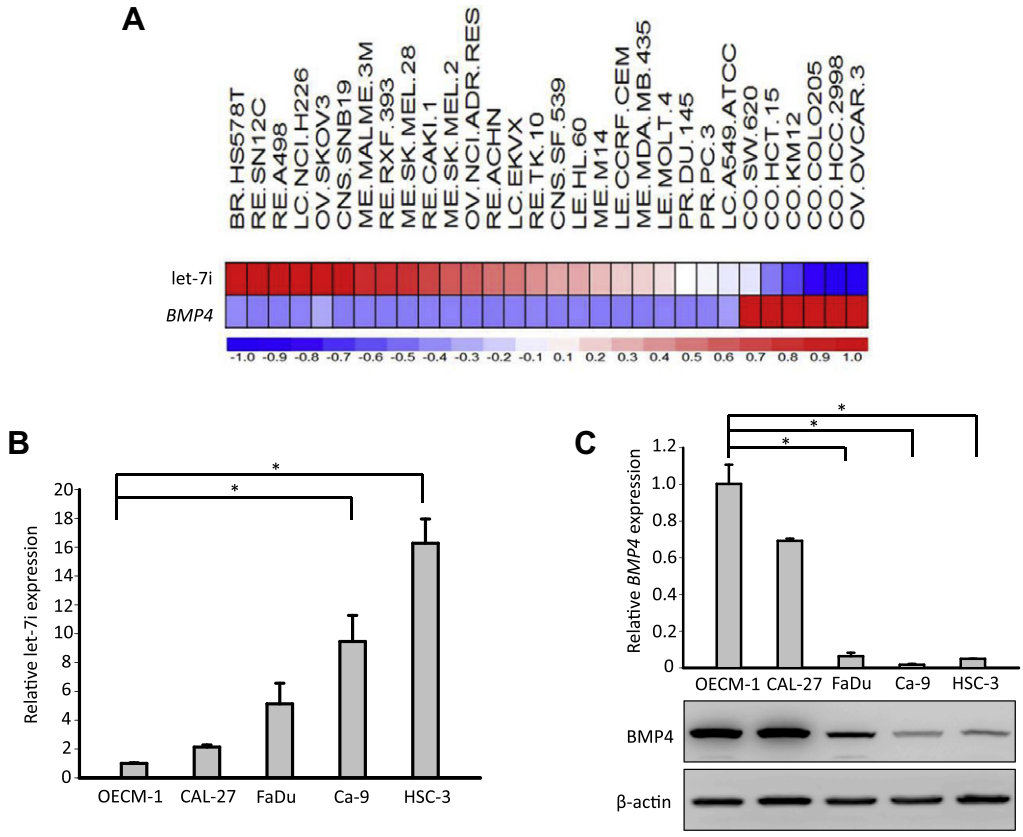

Fig. 1. The expression level of let-7i is inversely associated with BMP4 among different cancer cells. (A) A heatmap showing the relative expression let-7i and *BMP4* among 30 different cancer cell lines from NCI-60 panel. Red, upregulation; blue, downregulation. (B) Quantitative RT-PCR analysis of let-7i expression in five HNSCC cell lines ($n = 3$). Data represent mean ± SEM. $^{*}P < 0.05$ by Student's *t*-test. (C) Quantitative RT-PCR ($n = 3$) and western blot for analyzing the expression of BMP4 in five HNSCC cell lines. Data represent mean ± SEM. $^{*}P < 0.01$ by Student's *t*-test. (For interpretation of the references to color in this figure legend, the reader is referred to the web version of this article.)

was calculated as follows: [perimeter^2/4π(area)]. For a round cell, the ratio is 1, and an elongated cell would have an elevated index. For each clone, the mean value of the index was determined by calculating 100 cells.

2.9. 3D invasion assay

The method was described previously [18]. Briefly, after harvested cells attached in the Lab-Tek® chambered #1.0 coverglass system (#155383, Thermo Fisher Scientific, Waltham, MA), collagen solution (1.7 mg/ml) was loaded and polymerized at 37 °C in 10% CO_2 for 1 h. Medium containing 15% FBS was added as a chemoattractant. After incubation for 48 h, the cells were fixed and stained with Alexa-488 coupled to phalloidin. Confocal Z sections were collected from each well at 50 μm from the bottom of the well using a laser confocal microscope. For 3D imaging of the invaded cells, sequential Z sections were obtained and reconstructed using Olympus FV10-ASW 1.7 software. The invasion index was calculated as the number of cells at 30 μm divided by the total number of cells and was normalized by the proliferation index of each clone. The data are presented as the percentage of the invasion index of the control clone indicated in each panel.

2.10. Calculating the relative expression of the target transcripts in patient samples

We used GAPDH or U6 as the internal control to normalize the expression level of target molecules in each sample, and then calculated the tumor/normal ratio to represent the relative expression of each transcript ($2^{-\Delta\Delta CT}$).

2.11. Statistical analysis

Two-tailed independent Student's *t*-test was used to compare the continuous variables between two groups. The chi-square test was applied to compare the dichotomous variables. The level of statistical significance was set at 0.05 for all tests.

3. Results

3.1. The expression of let-7i inversely correlates with BMP4

We initially aimed to identify the novel let-7i target gene(s) that regulate(s) cellular migration because we previously found that let-7i represses mesenchymal-mode movement in HNSCC [18]. The cancer miRNA Regulatory Network (http://cmrn.systemsbiology.net/) [23] was applied to predict candidate targets of let-7i. We found that BMP4, a morphogenic protein that is critically involved in development and cancer progression [19,24–31], is a putative target of let-7i. Analysis of the microarray data from the NCI-60 database revealed an inverse correlation between expression levels of let-7i and BMP4 (Fig. 1A). Because the NCI-60 panel does not contain HNSCC cell lines, we examined the level of let-7i and determined BMP4 mRNA and protein levels in five HNSCC cell lines, OECM-1, CAL-27, FaDu, Ca-9 and HSC-3. The result showed that the level of endogenous let-7i negatively correlated with BMP4

mRNA and protein expression (Fig. 1B and C). These results suggest that let-7i expression is inversely correlated with BMP4 among different cancer cell lines, including HNSCC.

3.2. let-7i represses BMP4 expression through targeting the 3′-UTR of BMP4

To test whether BMP4 was indeed repressed by let-7i in HNSCC cell lines, we examined the protein and mRNA levels of BMP4 in OECM-1 cells with stable expression of a let-7i expression vector (OECM1-let7i) or a control vector (OECM1-mCherry) [18]. The results showed that downregulation of BMP4 was shown in OECM1-let7i cells (Fig. 2A). Next, we confirmed BMP4 as a direct target of let-7i. We inserted the human 3′-UTR of *BMP4* containing a let-7i binding site defined by MicroCosm Targets (http://www.ebi.ac.uk/enright-srv/microcosm/cgi-bin/targets/v5/mirna.pl) into the 3′-end of the luciferase gene to generate the reporter constructs. The sequence of the let-7i binding site in the 3′-UTR of BMP4 was completely conserved among different species (Fig. 2B). A reporter assay showed that the luciferase activity was suppressed in HEK-293T cells transfected with pmCherry-let-7i, and mutation of the let-7i binding site restored the activity (Fig. 2C). Transfection of a let-7i-neutralizing vector (pmCherry-spg-let7i) upregulated the luciferase activity in the wild-type *BMP4* reporter but not in the mutant reporter (Fig. 2D). These results confirm that BMP4 is a target that is repressed by let-7i.

3.3. Repression of BMP4 decreases mesenchymal migration in HNSCC

Because let-7i expression reduces cancer migration by repressing mesenchymal migration in 3D environments [18], and BMP4 is a direct target of let-7i, we investigated whether repression of BMP4 contributes to HNSCC migration in 3D systems by influencing individual cell movement. First, we infected two different shRNA sequences against *BMP4* and a control sequence into OECM-1 cells owing to the higher endogenous BMP4 levels in OECM-1 and our previous study showing that mesenchymal movement is the major movement mode in OECM-1 [18]. The knockdown effect of the two shRNAs was confirmed (Fig. 3A). F-actin immunofluorescent staining for cells cultured on top of collagen showed that the OECM-1 control cells had an elongated morphology. However, knockdown of BMP4 in OECM-1 cells changed the morphology to a round one (Fig. 3B). Quantification of cellular morphology by the equation [perimeter^2/4π(area)] confirmed that suppression of BMP4 in OECM-1 cells changed the 3D morphology to a round shape (Fig. 3C). This result was very similar to our previous finding that ectopic let-7i in OECM-1 cells changed the cell morphology from an elongated shape to a round one [18]. To

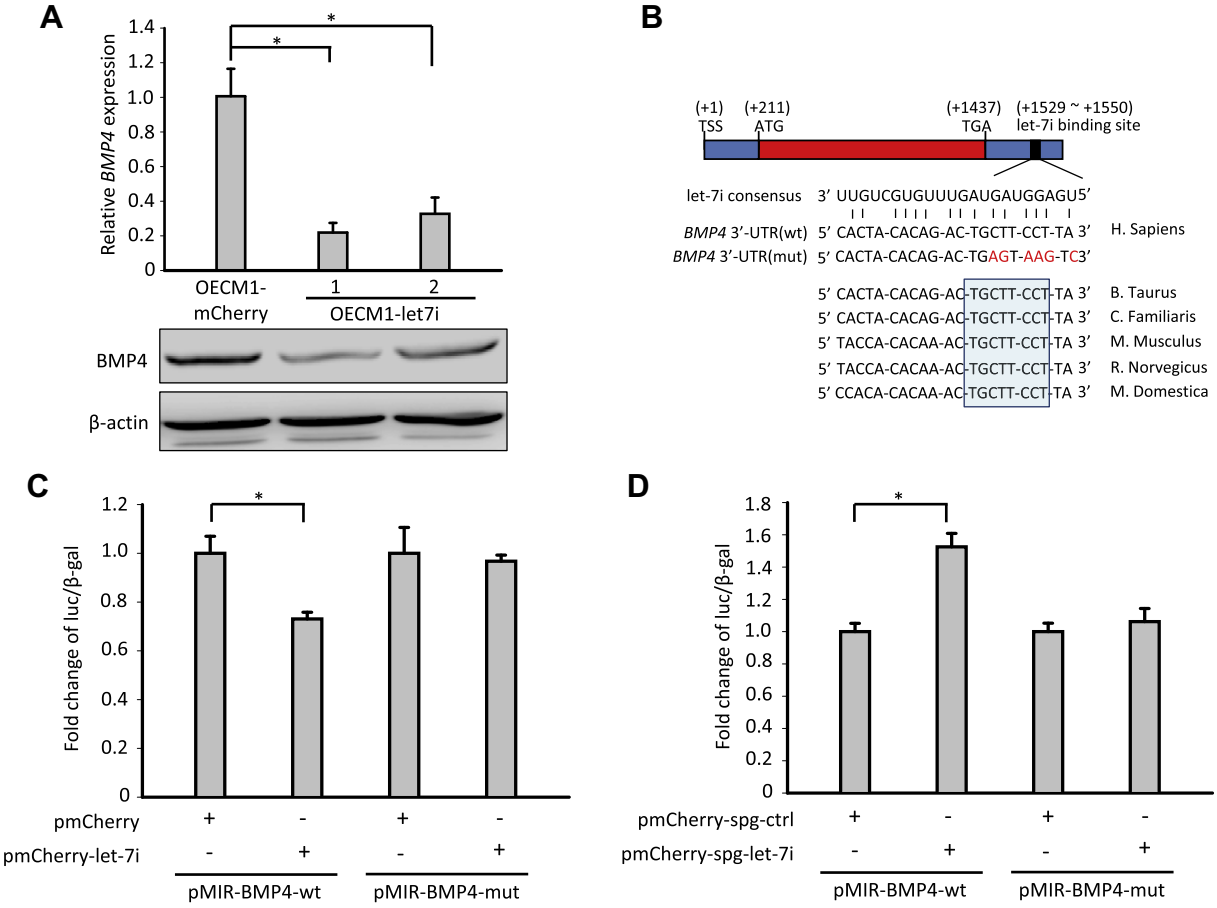

Fig. 2. let-7i directly represses BMP4 by targeting *BMP4* 3′-UTR. (A) Quantitative RT-PCR ($n = 3$) and western blot for analyzing BMP4 expression in OECM-1 cells transfected with a let-7i expression vector (OECM1-let-7i) or a control vector (OECM1-mCherry). Data represent mean ± SEM. $^*P < 0.05$ by Student's *t*-test. (B) Schematic representation of the 3′-UTR reporter constructs of wild-type *BMP4* (pMIR-BMP4-wt) and mutation of let-7i-binding seed region (pMIR-BMP4-mut). The conservation of the let-7i-binding seed region between different species is shown. (C) Luciferase reporter assay ($n = 3$ for each group). HEK-293T cells were co-transfected with a 3′-UTR reporter construct (pMIR-BMP4-wt/pMIR-BMP4-mut) and the let-7i expression vector (pmCherry-let7i) or an empty vector (pmCherry). Luciferase activity/β-galactosidase of cells transfected with pmCherry was applied as the baseline control for the experiments using the same reporter. Data represent mean ± SEM. $^*P < 0.05$ by Student's *t*-test. (D) Relative luciferase activity of HEK-293T cells co-transfected with a 3′-UTR reporter construct (pMIR-BMP4-wt/pMIR-BMP4-mut) and the let-7i neutralization vector (pmCherry-spg-let7i) or a control vector (pmCherry-spg-ctrl). Data represent mean ± SEM. $^*P < 0.05$ by Student's *t*-test.

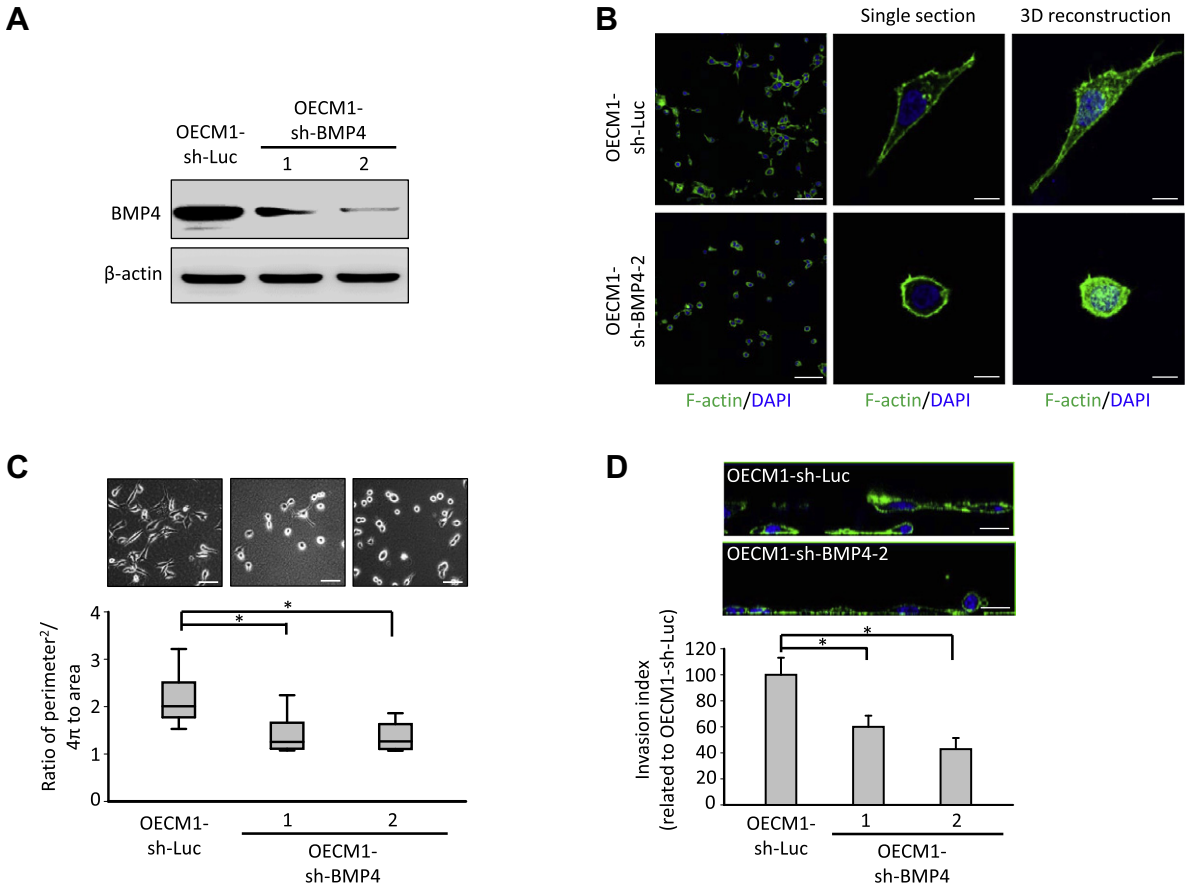

Fig. 3. Knockdown of BMP4 in OECM-1 reduces mesenchymal migration and represents a round morphology on top of collagen. (A) Western blot of BMP4 in OECM-1 cells receiving two different shRNA against BMP4 (OECM1-sh-BMP4-1 and 2) or a control sequence (OECM1-sh-Luc). β-Actin was used as a loading control. (B) Immunofluorescent staining and confocal microscopy to show the morphology and actin organization in OECM1-sh-BMP4 versus OECM1-sh-Luc. The green color indicates the F-actin stained by an anti-phalloidin antibody, and blue color indicates the nuclei stained by DAPI. Scale bar = 100 μm (first line), 10 μm (second and third line). (C) Upper: phase-contrast images of OECM1-sh-BMP4 clones and OECM1-sh-Luc. Scale bar = 25 μm. Lower: quantification of cellular morphology in OECM1-sh-BMP4 clones and OECM1-sh-Luc. The morphologic index was calculated as perimeter^2/4π to area. (n = 200 for each cell line) $^*P < 0.01$ by Student's t-test. (D) 3D invasion assay. Representative images of OECM1-sh-BMP4 and OECM1-sh-Luc invaded into collagen after 48 h (upper) and the relative invasion index (lower; n = 3). $^*P < 0.01$ by Student's t-test. Scale bar, 20 μm. (For interpretation of the references to color in this figure legend, the reader is referred to the web version of this article.)

examine whether repression of BMP4 could reduce mesenchymal migration in 3D environments, 3D invasion assays were performed. A significant reduction in the invasion index in OECM1-sh-BMP4 cells compared with the control cells was shown (Fig. 3D). Taken together, these data indicate that in OECM-1 cells, repression of BMP4 changes the cell morphology to a round shape and reduces mesenchymal movement.

3.4. Correlation of let-7i and BMP4 in the HNSCC specimens

Next, we confirmed the repression of *BMP4* by let-7i in HNSCC patient samples. Quantitative RT-PCR was used to analyze the expression levels of let-7i and *BMP4* in 40 HNSCC samples. The result showed that nearly half of the samples showed a let-7i^{low}-*BMP4*^{high} profile (Fig. 4A), a finding that is consistent with our *in vitro* results. Further analysis of the relative expression level showed a significant negative correlation between let-7i and *BMP4* in these HNSCC samples (Fig. 4B). These results confirm the existence of let-7i-BMP4 signaling in HNSCC patients.

4. Discussion

BMP4 is a morphogenic protein that plays an important role in embryogenesis and stem cell development [19,24]. The significance of BMP4 in cancer cells has been highlighted recently: increased expression of BMP4 has been shown in different types of cancers, including melanoma, ovarian carcinoma, gastric carcinoma, hepatocellular carcinoma, renal cell carcinoma and HNSCC [25–31], and increased BMP4 expression is associated with a worse outcome of HNSCC [29]. Recent studies have also suggested that BMP4 can increase migration and invasion in pancreatic cancer and colorectal cancer [32,33]. However, the impact of BMP4 on cancer cells 3D migration has never been addressed. In the present study, we demonstrate that suppression of BMP4 in mesenchymal-type HNSCC cells reverses the cell morphology to a round one and reduces the ability to migrate in a 3D environment. This result clarifies the biological significance of BMP4 in cancer migration. However, the mechanism of BMP4-induced migration in the 3D system is still unclear and requires further investigation.

let-7 family microRNAs are well-known tumor suppressors that function through repressing stem cell properties and tumorigenicity [17]. However, the role of let-7 in cancer migration is poorly defined. Our previous study discovered a novel function of let-7i in cancer migration: let-7i represses mesenchymal-mode movement through targeting the RAC1 co-activators NEDD9 and DOCK3 without counter-activation of amoeboid-mode movement. This molecular event leads to repression of local invasion in HNSCC [18]. In the present study, we further identify a new let-7i target responsible for cellular migration, BMP4. Together with our previous finding,

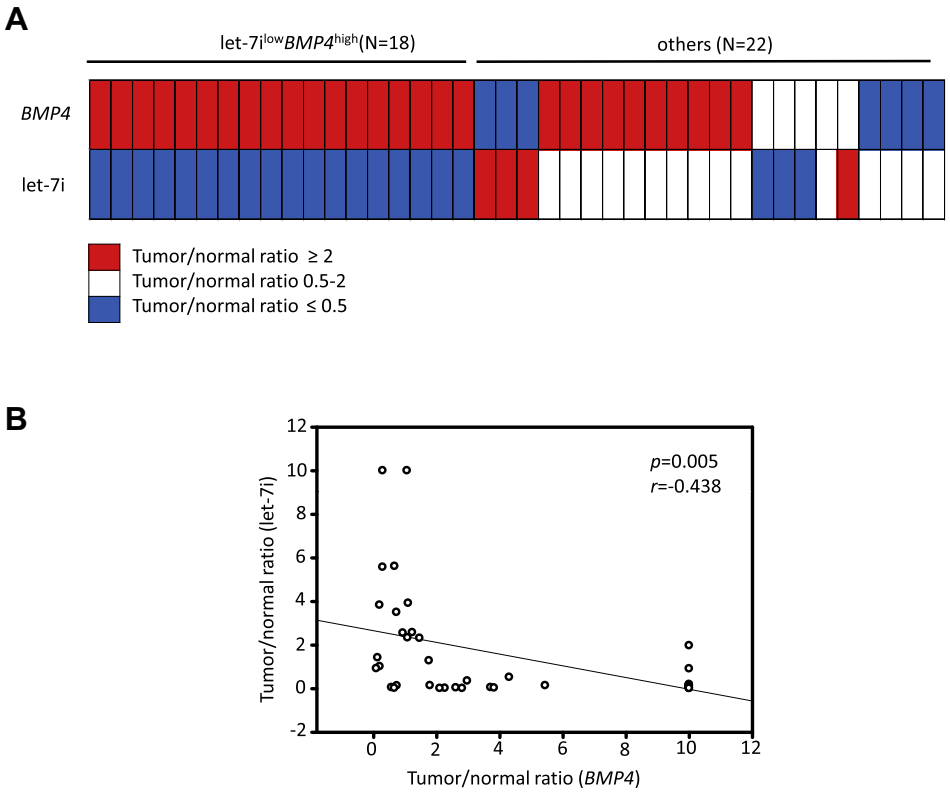

Fig. 4. Inverse correlation between let-7i and *BMP4* in HNSCC samples. (A) A heatmap showing the expression of *BMP4* and let-7i in HNSCC samples ($n = 40$). Red, upregulation in tumor tissue (tumor/normal $\geqslant 2$); blue, downregulation in tumor tissue (tumor/normal $\leqslant 0.5$); white: tumor/normal mRNA expression ratio between 0.5 and 2. (B) Relative expression (tumor/normal) of let-7i and *BMP4* in HNSCC samples. The correlation coefficient *r* and the *P* value are shown in the panel. (For interpretation of the references to color in this figure legend, the reader is referred to the web version of this article.)

we suggest that let-7i represses cellular migration in 3D environments through simultaneously targeting different genes, including *NEDD9*, *DOCK3*, and *BMP4*. Reduced expression of let-7i in HNSCC results in upregulation of these migration-related let-7i targets, which act in concert to promote HNSCC migration.

In the present study, we found that the let-7i binding site on the human *BMP4* 3′-UTR (5′-CTTCCTTA-3′) is highly conserved among different species, implicating that let-7i may repress BMP4-related functions among various biological conditions in addition to cancer cells. Because the let-7 family is also expressed late in mammalian embryonic development and regulates key differentiation processes during development [16], our study indicates that the regulation of BMP4 by let-7i may also play a role in vertebrate development. Further studies to define the significance of the let-7i-BMP4 axis in development and stem cells are necessary.

In summary, our study discovered a novel let-7i target in cancer migration—i.e., BMP4—and demonstrated a novel function of BMP4 in the 3D movement of cancer cell. These results will be valuable for understanding the role of BMP4 in cancer invasion and reinforce that let-7i is a potential therapeutic molecule for inhibiting local invasion in HNSCC.

Acknowledgments

This work was supported by National Health Research Institutes (NHRI-EX100-10037BI to M.H.Y.), National Science Council (101-2321-B-010-007 to M.H.Y.), Taipei Veterans General Hospital (V102-E8-002; V102C-036 to M.H.Y.), a grant from Ministry of Education, Aim for the Top University Plan (to M.H.Y.), and a grant from Department of Health, Center of Excellence for Cancer Research (DOH101-TD-C-111-007 to M.H.Y).

References

[1] A. Jemal, R. Siegel, J. Xu, et al., Cancer statistics, CA Cancer J. Clin. 60 (2010) 277–300.
[2] D. Goldenberg, J. Lee, W.M. Koch, et al., Habitual risk factors for head and neck cancer, Otolaryngol. Head Neck Surg. 131 (2004) 986–993.
[3] W. Garavello, A. Ciardo, R. Spreafico, et al., Risk factors for distant metastases in head and neck squamous cell carcinoma, Arch. Otolaryngol. Head Neck Surg. 132 (2006) 762–766.
[4] S. Evan-Ram, K.M. Yamada, Cell migration in 3D matrix, Curr. Opin. Cell Biol. 17 (2005) 524–532.
[5] E.M. Slorach, J. Chou, Z. Werb, Zepp o1 is a metastasis promoter that represses E-cadherin expression and regulates p120-catenin isoform expression and localization, Genes Dev. 25 (2011) 471–484.
[6] K. Wolf, Y.I. Wu, Y. Liu, et al., Multi-step pericellular proteolysis controls the transition from individual to collective cancer cell invasion, Nat. Cell Biol. 9 (2007) 893–904.
[7] P. Friedl, K. Wolf, Plasticity of cell migration: a multiscale tuning model, J. Cell Biol. 188 (2010) 11–19.
[8] V. Sanz-Moreno, G. Gadea, J. Ahn, et al., Rac activation and inactivation control plasticity of tumor cell movement, Cell 135 (2008) 510–523.
[9] V. Sanz-Moreno, C.J. Marshall, The plasticity of cytoskeletal dynamics underlying neoplastic cell migration, Curr. Opin. Cell Biol. 22 (2010) 690–696.
[10] K. Panková, D. Rösel, M. Novotný, et al., The molecular mechanisms of transition between mesenchymal and amoeboid invasiveness in tumor cells, Cell. Mol. Life Sci. 67 (2010) 63–71.
[11] D.P. Bartel, MicroRNAs: genomics, biogenesis, mechanism, and function, Cell 116 (2004) 281–297.
[12] M.V. Iorio, C.M. Croce, MicroRNAs in cancer: small molecules with a huge impact, J. Clin. Oncol. 27 (2009) 5848–5856.
[13] J. Lu, G. Getz, E.A. Miska, et al., MicroRNA expression profiles classify human cancers, Nature 435 (2005) 834–838.
[14] D.M. Dykxhoorn, MicroRNAs and metastasis: little RNAs go a long way, Cancer Res. 70 (2010) 6401–6406.
[15] N.S. Sokol, P. Xu, Y.N. Jan, et al., Drosophila let-7 microRNA is required for remodeling of the neuromusculature during metamorphosis, Genes Dev. 22 (2008) 1591–1596.
[16] E.E. Caygill, L.A. Johnston, Temporal regulation of metamorphic processes in Drosophila by the let-7 and miR-125 heterochronic microRNAs, Curr. Biol. 18 (2008) 943–950.

[17] M.E. Peter, Let-7 and miR-200 microRNAs: guardians against pluripotency and cancer progression, Cell Cycle 8 (2009) 843–852.
[18] W.H. Yang, H.Y. Lan, C.H. Huang, et al., RAC1 activation mediates Twist1-induced cancer cell migration, Nat. Cell Biol. 14 (2012) 366–374.
[19] B.L. Hogan, Bone morphogenetic proteins: multifunctional regulators of vertebrate development, Genes Dev. 10 (1996) 1580–1594.
[20] W.C. Reinhold, M. Sunshine, H. Liu, et al., Cell Miner: a web-based suite of genomic and pharmacologic tools to explore transcript and drug patterns in the NCI-60 cell line set, Cancer Res. 72 (2012) 3499–3511.
[21] C. Chen, D.A. Ridzon, A.J. Broomer, et al., Real-time quantification of microRNAs by stem-loop RT-PCR, Nucleic Acids Res. 33 (2005) e179.
[22] C.H. Huang, W.H. Yang, S.Y. Chang, et al., Regulation of membrane-type 4 matrix metalloproteinase by SLUG contributes to hypoxia-mediated metastasis, Neoplasia 11 (2009) 1371–1382.
[23] C.L. Plaisier, M. Pan, N.S. Baliga, A miRNA-regulatory network explains how dysregulated miRNAs perturb oncogenic processes across diverse cancers, Genome Res. 22 (2012) 2302–2314.
[24] M.A. Vicente López, M.N. Vázquez García, A. Entrena, et al., Low doses of bone morphogenetic protein 4 increase the survival of human adipose-derived stem cells maintaining their stemness and multipotency, Stem Cells Dev. 20 (2011) 1011–1019.
[25] J.B. Sneddon, H.H. Zhen, K. Montgomery, et al., Bone morphogenetic protein antagonist gremlin 1 is widely expressed by cancer-associated stromal cells and can promote tumor cell proliferation, Proc. Natl. Acad. Sci. 103 (2006) 14842–14847.
[26] C. Kwak, Y.H. Park, I.Y. Kim, et al., Expression of bone morphogenetic proteins, the subfamily of the transforming growth factor-beta superfamily, in renal cell carcinoma, J. Urol. 178 (2007) 1062–1067.
[27] S.G. Kim, H.R. Park, S.K. Min, et al., Expression of bone morphogenic protein-4 is inversely related to prevalence of lymph node metastasis in gastric adenocarcinoma, Surg. Today 41 (2011) 688–692.
[28] L. Laatio, P. Myllynen, R. Serpi, et al., BMP-4 expression has prognostic significance in advanced serous ovarian carcinoma and is affected by cisplatin in OVCAR-3 cells, Tumour Biol. 32 (2011) 985–995.
[29] T. Xu, C.Y. Yu, J.J. Sun, et al., Bone morphogenetic protein-4-induced epithelial–mesenchymal transition and invasiveness through Smad1-mediated signal pathway in squamous cell carcinoma of the head and neck, Arch. Med. Res. 42 (2011) 128–137.
[30] C.Y. Chiu, K.K. Kuo, T.L. Kuo, et al., The activation of MEK/ERK signaling pathway by bone morphogenetic protein 4 to increase hepatocellular carcinoma cell proliferation and migration, Mol. Cancer Res. 10 (2012) 415–427.
[31] T. Rothhammer, I. Poser, F. Soncin, et al., Bone morphogenic proteins are overexpressed in malignant melanoma and promote cell invasion and migration, Cancer Res. 65 (2005) 448–456.
[32] K.J. Gordon, K.C. Kirkbride, T. How, et al., Bone morphogenetic proteins induce pancreatic cancer cell invasiveness through a Smad1-dependent mechanism that involves matrix metalloproteinase-2, Carcinogenesis 30 (2009) 238–248.
[33] H. Deng, T.S. Ravikumar, W.L. Yang, Overexpression of bone morphogenetic protein 4 enhances the invasiveness of Smad4-deficient human colorectal cancer cells, Cancer Lett. 281 (2009) 220–231.